

This article was downloaded by:[Bochkarev, N.]
On: 19 December 2007
Access Details: [subscription number 788631019]
Publisher: Taylor & Francis
Informa Ltd Registered in England and Wales Registered Number: 1072954
Registered office: Mortimer House, 37-41 Mortimer Street, London W1T 3JH, UK



Astronomical & Astrophysical Transactions

The Journal of the Eurasian Astronomical Society

Publication details, including instructions for authors and subscription information:
<http://www.informaworld.com/smpp/title~content=t713453505>

Anisotropic stellar winds in binary systems

I. Pustynnik^a

^a Tartu Astrophysical Observatory, Tõravere, Estonia

Online Publication Date: 01 January 1994

To cite this Article: Pustynnik, I. (1994) 'Anisotropic stellar winds in binary systems',

Astronomical & Astrophysical Transactions, 5:1, 287 - 301

To link to this article: DOI: 10.1080/10556799408245880

URL: <http://dx.doi.org/10.1080/10556799408245880>

PLEASE SCROLL DOWN FOR ARTICLE

Full terms and conditions of use: <http://www.informaworld.com/terms-and-conditions-of-access.pdf>

This article maybe used for research, teaching and private study purposes. Any substantial or systematic reproduction, re-distribution, re-selling, loan or sub-licensing, systematic supply or distribution in any form to anyone is expressly forbidden.

The publisher does not give any warranty express or implied or make any representation that the contents will be complete or accurate or up to date. The accuracy of any instructions, formulae and drug doses should be independently verified with primary sources. The publisher shall not be liable for any loss, actions, claims, proceedings, demand or costs or damages whatsoever or howsoever caused arising directly or indirectly in connection with or arising out of the use of this material.

ANISOTROPIC STELLAR WINDS IN BINARY SYSTEMS

I. PUSTYLNİK

Tartu Astrophysical Observatory, Tõravere, EE2444, Estonia

(Received April 13, 1993)

Implications of the displacement of a sonic point due to the presence of a companion in a binary system for the properties of anisotropic stellar wind are studied for adiabatically expanding stellar wind. A mass flux tube is introduced for the evaporative wind and examined for characteristic temperatures of gas in the framework of the Roche model. Accretion radii values are tabulated for different values of the mass ratio and the ratio of the local sonic velocity to the escape velocity of gas. An explicit upper limit estimate T_0 of gas temperature is introduced such that for T less than T_0 conditions for transonic flow are fulfilled. The effect of optically thin anisotropic wind upon the light curves of eclipsing variables is quantitatively evaluated.

KEY WORDS Close binaries – stellar wind, mass loss and mass transfer

1 INTRODUCTION

During the last two decades the peculiarities of stellar winds in close binary systems have been discussed in a number of papers (Basko and Sunyaev, 1973; McCray and Hatchett, 1975; Kolychalov and Sunyaev, 1979; Friend and Castor, 1982; Hadrava, 1985; Ivanov, 1987; etc.). More recently a quantitative treatment of stellar wind for a non-spherical medium has been proposed (see, for instance, Chen Fusheng, 1989; de Araujo and de Freitas Pacheco, 1989; Mazzali, 1991).

New observational data point to the existence of various types of inhomogeneities of circumstellar material. Thus, in some Algol-type systems where full eclipses provide an exceptional opportunity of detailed study in morphology and dynamics of ambient gas, several peculiar features in its behaviour have been discovered; i) asymmetry between the leading and the trailing hemispheres of the mass gaining component; ii) regions emitting in continuum and in spectral lines are loosely spatially correlated; iii) velocity field is strikingly different from the Keplerian one, etc. (for more details see Kaitchuck and Honeycutt, 1982; Kaitchuck, 1989). Most probably, these inhomogeneities should result, at least partially, from the stellar wind.

The concept of anisotropic stellar wind has been introduced and worked out in papers of McCray and Hatchett (1975), Friend and Castor (1982) and Hadrava

(1985). Following these papers we examine here some implications of a displacement of a sonic point in a binary system for a simple model of evaporative stellar wind for the Roche model.

The importance of studying the consequences of anisotropic stellar wind is underscored by the fact that in very many close binaries for which reliable photometric and spectroscopic elements are available classical accretion discs cannot be formed in view of redundant angular momentum of the accreting matter (Lubow and Shu, 1975). Recently Tout and Hall (1991) proposed several arguments favouring the idea that bona fide stellar wind may be a driving mechanism governing mass transfer if the time-scale for radius changes following mass loss is much shorter than for the radius changes owing to nuclear evolution. As it will be indicated below, anisotropy of stellar wind opens up an opportunity to assess a better mass transfer rate directly from the light curves provided the rate is sufficient to produce an observable effect upon the light curve. Generalization of available models for the case of the optically thick wind should give a better insight into the problems of the present status and the evolution of early type contact systems which are still far from being properly understood.

2 ANISOTROPIC STELLAR WIND: EQUATIONS FOR WIND EXPANSION ZONE AND SOLUTION

For a stationary flow, ignoring the Coriolis forces due to stellar rotation, the equation of motion of gas and the equation of continuity look as follows

$$(\vec{u}\nabla)\vec{u} + \nabla\Phi + \frac{1}{\rho}\nabla P = 0, \quad (1)$$

$$\nabla(\rho\vec{u}) = 0. \quad (2)$$

Here \vec{u} is the gas velocity, ρ and P are, respectively, the local density of matter and the pressure exerted by both gas and radiation, Φ is the gravitational potential. Eq. (1) is a good approximation provided that $u_s/u_{orb} \ll 1$ where u_s is the local sound velocity and u_{orb} is the velocity of orbital motion. We shall treat here an idealized case of radial adiabatic expansion of gas from a one component of a binary.

In this case Eq. (2) reduces to the conservation of mass flux (mass flow rate per unit solid angle) along the streamline, i.e.,

$$J = \rho u R^2 = \text{const} \quad (3)$$

and Eq. (1) reduces to

$$u \frac{du}{dR} = -\frac{1}{\rho} \frac{dP}{dR} - \frac{d\Phi}{dR}. \quad (4)$$

Introducing the gravitational potential of the Roche model, using Eq. (3) and the relation between gas pressure and matter density valid for adiabatic process

$P = K\rho^\gamma$ one obtains

$$\frac{1}{2} \left(1 - \frac{u_s^2}{u^2} \right) \frac{du^2}{dR} = \frac{2}{R} u_s^2 - \frac{d\Phi}{dR}, \quad (5)$$

where u_s is the local sound velocity.

Let us specify what we are going to investigate subsequently and the limitations involved. Suppose that the term dP/dR in Eq. (4) would include the radiative force in spectral lines proportional to $\sigma\rho u \left| \frac{du}{dR} \right|^{-1}$ where σ is the electron scattering cross section and du/dR the velocity gradient. In that case, we would have conventional equation of radiative stellar wind treated in a number of papers quoted above, specifically by Friend and Castor (1982). The spatial extent of the wind formation zone (chromosphere) is small, at most $10^{-3} - 10^{-2} a$, where a is the semi-major axis of the orbit. Beyond that zone, the influence of forces other than gravitation and gas pressure quickly diminishes. This is the physical reason behind the definition of the 'central core' and 'halo' of the wind (Mihalas, 1978; Castor *et al.*, 1975). In our subsequent treatment we focus our attention on this extended region that we would call the expanding wind zone and look more closely at the effects of anisotropy caused by the presence of the secondary component.

From now on we shall consider for the sake of simplicity a two-dimensional case and introduce the gravitational potential, given by

$$\begin{aligned} \Phi = & \frac{GM_1}{R} + \frac{GM_2}{\sqrt{a^2 - 2aR\mu + R^2}} + \frac{G(M_1 + M_2)}{2a^3} \\ & \times \left[R^2 - \frac{2M_2}{M_1 + M_2} R\mu + \left(\frac{M_2}{M_1 + M_2} \right)^2 \right] \end{aligned} \quad (6)$$

at the equatorial plane. G is the gravitation constant, M_1 , M_2 are the masses of mass losing and mass accreting components, respectively, μ is the cosine of angle between the line joining the centres of two stars and the direction considered in the equatorial plane from the centre of mass losing component. To facilitate the derivation of subsequent formulae, we express the radial velocity in dimensionless units $v = u/u_e$ where $u_e = \sqrt{\frac{2G(M_1+M_2)}{a}}$ and we introduce a dimensionless potential $C = \frac{\Phi a}{G(M_1+M_2)}$ (Plavec and Kratochvil, 1964) and express R in units of a . Thus we obtain

$$\frac{1}{2} \left(1 - \frac{v_s^2}{v^2} \right) \frac{dv^2}{dr} = \frac{2}{r} v_s^2 - \frac{dC}{dr},$$

and

$$\frac{dC}{dr} = \frac{1}{1+q} \left[-\frac{1}{r^2} + q \frac{\mu - r}{(1 - 2r\mu + r^2)^{3/2}} + \left(r - \frac{q}{1+q} \mu \right) (1+q) \right]. \quad (7)$$

In the latter equation, q is the mass ratio. In Eq. (7), μ is treated as a parameter. Actually the absence of another equation involving $\frac{dv}{d\mu}$ in addition to Eq. (7) implies

that we assume simply $v_\mu \ll v_r$ opposite to the case of accretion disc theory where ordinarily just the opposite is supposed, i.e., $v_\mu \gg v_r$.

We examine now more closely the anisotropy of the stellar wind due to the secondary component. Denoting the coordinates of the sonic points r'_s and r''_s for $\mu = 1$ and $\mu = -1$, respectively ($\mu = 1$ corresponding to the direction towards mass accreting component and $\mu = -1$ to the opposite one), we find from Eq. (7) the radial difference $\Delta r_s = r'_s - r''_s$ of the equatorial sonic point coordinates due to the presence of the companion star

$$\frac{\Delta r_s}{r_s} \simeq \frac{1}{4} f(r_s) q r_s^2 \frac{u_c^2}{u_s^2}, \quad (8)$$

where $r_s = \frac{1}{2}(r'_s + r''_s)$ and

$$f(r_s) = \frac{1}{(1+r_s)^2} + \frac{1}{(1-r_s)^2} - 2(1+q)r_s. \quad (9)$$

When deriving relation (8) we neglect the difference in sonic velocities u_s for $\mu = 1$ and $\mu = -1$ and take into account that $\Delta r_s/r_s \ll 1$. Since $r_s \simeq 0.1 - 0.3$ for typical binaries, $f(r_s) \sim 1$ and $u_c^2/u_s^2 \simeq 1$, one obtains $\Delta r_s/r_s \sim 10^{-3} - 10^{-2} a$ which for $a r_s = R_\odot$ implies the displacement $\Delta r_s \simeq 10^7$ cm, a value comparable to the scale of the chromosphere. Since the mass loss rate $\dot{M} = 4\pi\rho_s u_s r_s^2$ depends primarily on the gas density ρ which is very sensitive to the depth in the chromosphere (u_s scales as the square root of temperature but the accompanying change with the depth would be much smaller), the net result should be the higher mass flux in the direction pointing to the companion star.

A similar conclusion follows from the arguments connected with the mass flux conservation condition. Suppose that we deal with the evaporative stellar wind from a single star. Then for small Mach numbers one should have

$$J = \rho u R^2 = \rho_s u_s R_s^2 \exp^{-\frac{GM}{R_s kT}}. \quad (10)$$

By the same token we can suppose for the case of binary systems in a two-dimensional case considered here

$$J \sim \exp^{-\frac{\Phi_s}{kT_s}}, \quad (11)$$

where Φ_s is the effective potential including repulsive forces at the sonic point where solutions for subsonic and supersonic regimes should be matched. Combining relations (3) and (11) we have

$$J = \rho v r^2 = \frac{\dot{M}}{4\pi I(q, r_{os})} \exp\left[-\frac{v_c^2}{v_s^2} F(q, r_{os}, \mu)\right], \quad (12)$$

where $\dot{M} = \int J d\omega$ is the mass loss rate and

$$I(q, r_{os}) = \frac{1}{2} \int_{-1}^{+1} \exp\left[-\frac{v_c^2}{v_s^2} F(q, r_{os}, \mu)\right] d\mu,$$

$F(r_{os}, q, \mu)$ denotes the difference of dimensionless potentials C

$$F(r_{os}, q, \mu) = C(q, r_{os}, \mu) - C(q, r_{os}, \mu = 1),$$

and r_{os} is the coordinate of the sonic point for $\mu = 1$.

Both the velocity and density distributions should be found as a self-consistent solution of the set of Eqs (7), (12) with the equation of state valid for adiabatic expansion and the boundary conditions properly formulated. That will be done elsewhere. Here we confine our treatment of the problem to semi-quantitative estimates. Namely in what follows we shall indicate that formula (12) corresponds to stream tubes with different values of v_s/v_e for different types of flows. We examine here the location of the sonic points in the framework of the Roche model for some types of flows.

If the left-hand side of Eq. (7) equals zero then either $v = v_s$ or $\frac{dv}{dr}|_{r=r_s} = 0$ (the case when $v = v_s$ and $\frac{dv}{dr}|_{r=r_s} = \infty$ will not be considered here). Both former cases are physically justified. If $r_s \simeq r_{L_1}$, where r_{L_1} is the coordinate of the first Lagrangian point, then gravitational attraction of both components is counterbalanced and the velocity of gas would be minimum, at least for a free-fall case. On the other hand, in a supersonic flow v changes quite slowly so that $v \simeq v_s$ in the vicinity of the first Lagrangian point (Basko and Sunayev, 1973).

i) The case $v_s \ll v_e$. For $v_s \ll v_e$ zero points of the right-hand side of Eq. (7) coincide with the equipotentials of the Roche model.

It can be indicated that the zero points of the right-hand side of Eq. (7) forming closed curves around the mass gaining component (accretion circles) lie within the cone whose width can be found from the condition of contact, i.e., $\mu = r_0$. The respective radius R_{accr} may be called the radius of accretion from the stellar wind, i.e., $R_{\text{accr}} = \sqrt{1 - r_0^2}$ in the framework of our two-dimensional model and r_0 , as can be seen directly from Eq. (7), can be found as the real root of the following cubic equation:

$$r_0^3 + 2r_0(1+q)(v_s/v_e)^2 - 1 = 0, \quad (13)$$

for $v_s \ll v_e$ simply

$$r_0 = \left(\frac{1}{2} + F(q, v_s/v_e) \right)^{1/3} + \left(\frac{1}{2} - F(q, v_s/v_e) \right)^{1/3}, \quad (14)$$

where

$$F(q, v_s/v_e) = \left[\frac{1}{4} + \left[\frac{2}{3}(1+q) \frac{v_s^2}{v_e^2} \right]^3 \right]^{1/2}.$$

We have tabulated R_{accr} values as a function of the mass ratio q and v_s/v_e (Table 1). Note that for $v_s/v_e \simeq 0.16 - 0.23$ (depending on the mass ratio value q) R_{accr} exceeds the radius R_{L_1} of the Roche lobe, thereby setting an upper limit of v_s/v_e .

Table 1 Accretion radius R_{accr} as a function of mass ratio q and the ratio v_s/v_e

v_s/v_e	q				
	0.10	0.15	0.20	0.25	0.30
0.02	0.024	0.025	0.025	0.026	0.026
0.04	0.048	0.050	0.051	0.052	0.053
0.06	0.073	0.074	0.076	0.077	0.079
0.08	0.097	0.099	0.101	0.103	0.105
0.10	0.122	0.125	0.127	0.129	0.132
0.12	0.145	0.149	0.152	0.154	0.158
0.14	0.169	0.177	0.180	0.183	0.185
0.16	0.193	0.197	0.201	0.205	0.209
0.18	0.217	0.221	0.226	0.231	0.235
0.20	0.240	0.246	0.251	0.256	0.261
0.22	0.264	0.270	0.276	0.281	0.286
0.24	0.287	0.294	0.300	0.306	0.312
0.26	0.311	0.318	0.324	0.331	0.337
0.28	0.334	0.341	0.348	0.355	0.362
0.30	0.357	0.365	0.372	0.380	0.387

Table 1 Continued

v_s/v_e	q				
	0.35	0.40	0.45	0.50	0.55
0.02	0.027	0.027	0.028	0.028	0.029
0.04	0.054	0.055	0.056	0.057	0.058
0.06	0.080	0.082	0.083	0.083	0.085
0.08	0.107	0.109	0.110	0.111	0.115
0.10	0.133	0.137	0.138	0.144	0.144
0.12	0.161	0.164	0.166	0.169	0.172
0.14	0.187	0.190	0.194	0.197	0.200
0.16	0.213	0.217	0.221	0.225	0.229
0.18	0.240	0.244	0.248	0.252	0.257
0.20	0.266	0.271	0.275	0.280	0.284
0.22	0.292	0.297	0.302	0.307	0.312
0.24	0.318	0.323	0.329	0.334	0.345
0.26	0.343	0.349	0.355	0.361	0.373
0.28	0.369	0.375	0.382	0.389	0.394
0.30	0.394	0.401	0.407	0.414	0.420

Table 1 Continued

v_s/v_e	q				
	0.60	0.65	0.70	0.75	0.80
0.02	0.029	0.030	0.030	0.031	0.031
0.04	0.058	0.059	0.060	0.061	0.062
0.06	0.088	0.089	0.090	0.092	0.093
0.08	0.115	0.119	0.119	0.122	0.125
0.10	0.145	0.148	0.150	0.153	0.154
0.12	0.175	0.177	0.180	0.183	0.185
0.14	0.203	0.206	0.210	0.213	0.216
0.16	0.232	0.236	0.239	0.243	0.246
0.18	0.261	0.265	0.268	0.272	0.276
0.20	0.289	0.293	0.298	0.302	0.306
0.22	0.317	0.322	0.326	0.331	0.336
0.24	0.345	0.350	0.355	0.360	0.365
0.26	0.373	0.378	0.383	0.389	0.394
0.28	0.400	0.406	0.412	0.417	0.423
0.30	0.427	0.433	0.439	0.445	0.451

Table 1 Continued

v_s/v_e	q			
	0.85	0.90	0.95	1.00
0.02	0.031	0.032	0.032	0.033
0.04	0.063	0.064	0.065	0.065
0.06	0.094	0.095	0.097	0.098
0.08	0.125	0.127	0.129	0.130
0.10	0.156	0.158	0.161	0.163
0.12	0.188	0.190	0.193	0.195
0.14	0.219	0.221	0.224	0.227
0.16	0.249	0.253	0.256	0.259
0.18	0.280	0.283	0.287	0.291
0.20	0.310	0.314	0.318	0.322
0.22	0.340	0.345	0.349	0.353
0.24	0.370	0.375	0.379	0.384
0.26	0.399	0.404	0.409	0.414
0.28	0.428	0.434	0.439	0.444
0.30	0.457	0.463	0.468	0.474

Beyond this limit approximate Eq. (7) evidently loses its validity. For each binary with known M_1 , M_2 and a we may introduce gas temperature T_{Roche} such that

$$\overline{R_{L_1}} = R_{\text{accr}}(q, v_s/v_e), \quad (15)$$

R_{L_1} being the radius of the Roche lobe.

ii) $\frac{dv}{dr}\big|_{r=r_{L_1}} = 0$. Consider Eq. (7) at some point close to the first Lagrangian point $r_1 = \sqrt{r_{L_1}^2 \pm H^2}$ where $H = \sqrt{2}v_s(-dg_{\text{eff}}/dr)^{-1/2}r = r_{L_1}$ is the scale length for isothermal density drop-off of the gas flow at $r = r_{L_1}$. If one puts the right-hand side of Eq. (7) equal to zero one finds

$$T_0 = 5.73 \cdot 10^6 K \frac{(M_1 + M_2)_\odot}{(a/10R_\odot)} f_2(q, r_{L_1}, H),$$

$$f_2(q, r_{L_1}, H) = r_1 \left[-\frac{1}{(1+q)r_1^2} + \frac{q}{(1+q)(1-r_1^2)} + r_1 - \frac{q}{1+q} \right], \quad (16)$$

$H = 2v_s/v_e a k^{-1}$, where

$$k = \{f_3(q, r_{L_1}) [f_3(q, r_{L_1}) - 1]\}^{1/2},$$

$$f_3(q, r_{L_1}) = \frac{1}{(1+q)r_{L_1}^3} + \frac{q}{(1+q)(1-r_{L_1})^3}$$

so that $H/a \simeq v_s/v_e$ (Meyer and Meyer-Hoffmeister, 1983). In the vicinity of the first Lagrangian point the derivative $\frac{d\Phi}{dr}$ has a minimum. Thus relation (16) implies that if $T < T_0$ the right-hand side of Eq. (7) will be negative everywhere (except for a small region of a relative size H/a near L_1). In other words, for $T < T_0$ the conditions for transonic flow will be fulfilled since the velocity of the wind will be a growing function for subsonic velocity values and a decreasing one for supersonic velocities.

Finally one can introduce the minimum temperature T_{isotr} of isotropic evaporation (expansion) by setting simply the particle total energy (kinetic energy plus specific enthalpy minus the difference between the potentials at the surface of the mass losing component and the Roche critical potential) equal to zero. In our dimensionless units, we then have

$$v^2 + 5v_s^2 + C(q, \mu, r_1) - C_1(q) = 0, \quad (17)$$

where $C_1(q)$ is the value of the potential for the inner critical Roche lobe. Since the velocity does not change very drastically, one has

$$T_{\text{isotr}} \geq 3.82 \cdot 10^6 K \frac{(M_1 + M_2)_\odot}{(a/R_\odot)} \times \left[\frac{2}{(1+q)r_s} + \frac{2q}{1+q} \frac{1}{1-r_s} + \left(r_s - \frac{q}{1+q} \right)^2 - C_1(q) \right]. \quad (18)$$

Table 2 Characteristic temperatures T_0 , T_{isotr} and T_{Roche} for some binaries

System	$M_{1\odot}$	$M_{2\odot}$	a/R_\odot	$T_0/10^4$	$T_{\text{isotr}}/10^6$	$T_{\text{Roche}}/10^6$
V380 Cyg	13.3	7.6	62.2	2.0	2.9	0.4
V453 Cyg	16.8	12.9	32.2	6.8	4.3	1.1
VV Ori	10.2	4.5	13.4	4.0	3.3	0.6
δ Ori	23.0	9.0	43.0	33.5	1.9	0.8
V539 Ara	6.7	5.7	21.0	3.1	5.4	0.4
SZ Cam	20.4	5.1	24.0	12.5	3.8	0.6
TX Her	1.6	1.4	9.0	86.0	4.5	0.6
V448 Cyg	22.4	17.5	50.2	3.5	13.3	1.9
UW CMa	43.5	32.5	47.8	5.0	1.3	0.3
SV Cen	11.2	9.4	16.2	14.5	0.4	0.1
U Cep	4.3	2.8	14.8	9.5	5.5	1.0
RS Cep	1.9	0.7	31.4	4.5	3.3	0.5

We have calculated T_0 , T_{isotr} and T_{Roche} for some detached and semi-detached binaries, their values are indicated in the fifth, sixth and seventh columns of Table 2, respectively. Again we have set for the sake of simplicity $r_s = r_1$, r_1 being the radius of the mass losing component. Note that $T_0 < T_{\text{Roche}} < T_{\text{isotr}}$. T_{isotr} is in a good qualitative agreement with the temperatures of the coronal wind, T_{Roche} with the chromospheric temperatures and T_0 with the continuum data (evidence for the gas flows from light curves).

Figure 1 illustrates the behaviour of the mass flux as a function of μ calculated for three values v_s/v_e corresponding to the typical T_{isotr} , T_{Roche} and T_0 . It is noteworthy that the intermediate curve matches well the results for $J(\mu)$ obtained by Friend and Castor (1982) thereby implicitly confirming the validity of our model.

Different ad hoc flux tube approximations have been introduced in a number of papers, among others by Modisette and Kondo (1980), Haisch *et al.* (1980), and Kopp and Holzer (1976). From all the above-mentioned, it is clear that Eq. (12) may be regarded as an equation of a flux-tube based upon very simple but physically justified assumptions.

3 THE EFFECT OF ANISOTROPIC STELLAR WIND ON THE LIGHT CURVE OF AN ECLIPSING BINARY

We apply now the formulae derived above for optically thin stellar wind from one binary component and evaluate the mass transfer rate fitting the model and the observed light curves of detached binaries. Our schematic model is shown in Figure 3. Two stars with radii r_i revolve around the common centre of gravity in a circular orbit. Radially expanding stellar wind from the primary component forms a semi-transparent envelope of accreting matter whose size around the mass gaining star is R_{accr} (R_{accr} values are tabulated in Table 1), the size of the envelope around the primary $R_A = \sqrt{a^2 - 2a\delta(1 - \delta/a)}$, $\delta = \sqrt{R_{\text{accr}}^2 - H^2}$ is determined by R_{accr}

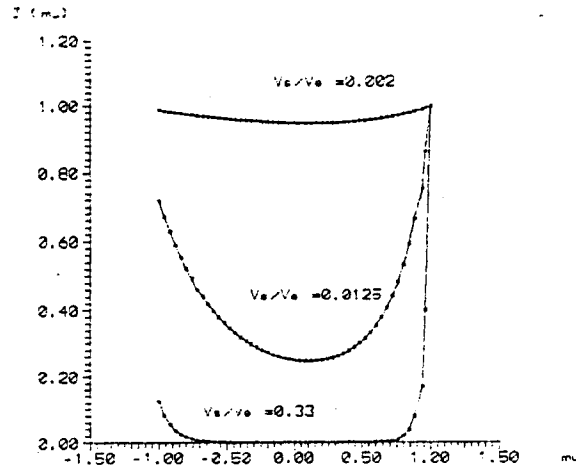


Figure 1 Different 'flux tubes' or angular dependencies of the mass flux J (mass loss rate per unit solid angle) for different ratios of sonic v_s to escape v_e velocities, $\mu = 1$ for the direction pointing towards the mass gaining component (for more details see the text).

and the size of the neck H connecting the two stars (see also Eq. (16)). In addition we suppose that i) the gas is fully ionized and scattering on free electrons is the predominant source of opacity; ii) both components are black body emitters with the effective temperatures $T_{\text{eff}1}$ and $T_{\text{eff}2}$; iii) stationary mass outflow takes place from the primary component at the mass loss rate \dot{M} . We neglect i) proximity effects for both components, ii) their finite sizes when calculating the optical depths of gas along the line of sight. We calculate the light curves with a due account for i) body eclipses by both components, ii) the screening effect of a semi-transparent scattering envelope and iii) the contribution of the latter into the total luminosity of a close binary.

When calculating the optical depth along the line of sight we need the density distribution which we find from Eq. (12), whereas the velocity distribution can be determined directly by integrating Eq. (7).

In view of the crudeness of our approach we have introduced subsequent simplifications: i) v_s is assumed to be constant (isothermal medium), ii) performing integration over μ in Eq. (12), we expand the exponential factor in series and retain terms up to r_{os}^2 which is sufficient for our purposes taking into account that $r_{\text{os}}^2 \ll 1$ and $\frac{q}{q+1} \simeq 0.2 - 0.3$ for detached binaries.

Thus we obtain the following expression for the density distribution:

$$\rho = \frac{\dot{M}}{4\pi I(q, r_{\text{os}}) v R^2} \exp \left[-\frac{v_e^2}{v_s^2} F(q, r_{\text{os}}, \mu) \right], \quad (19)$$

$$I(q, r_{\text{os}}) \simeq 1 - \frac{1}{2} \frac{q}{1+q} r_{\text{os}}^2 \frac{v_e^2}{v_s^2} - \frac{3}{4} \left(\frac{q}{1+q} \right)^2 p(r_{\text{os}}) \frac{v_e^4}{v_s^4},$$

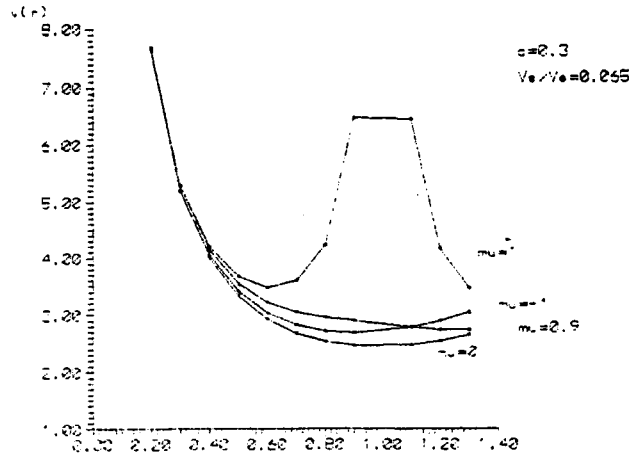


Figure 2a Velocity distributions for different values of μ , $q = 0.3$, cool gas, $v_s/v_e = 0.065$, $\mu = 1$ denotes the direction towards mass accreting component.

and

$$p(r_{os}) \simeq 1 - r_{os} \left[1 - \frac{4}{3(1 - r_{os})} \right] + \frac{1}{9} r_{os}^2 (1 + r_{os}) - \frac{1}{6 r_{os}} \ln \frac{1 - r_{os}}{1 + r_{os}}.$$

The velocity distribution for our case reads off

$$v^2 - v_s^2/v_e^2 \ln v^2 = 2v_s^2/v_e^2 \ln r^2 + C(r, \mu, q) + C_0, \tag{20}$$

where

$$C_0 = -v_s^2/v_e^2 \{ 5 + \ln [C_1(q) - 5v_s^2/v_e^2] r_{L_1}^4 \} \tag{21}$$

is the integration constant fixed by postulating the total particle energy at the first Lagrangian point to be zero. Thus fixing the integration constant we fix the velocity distribution of a supersonic flow for $r > r_s$. Two limiting cases have been considered here: i) cool gas, $v_s \ll v_e$, $T \simeq T_0$ (see Eq. (16)), ii) hot gas, $v_s^2/v_e^2 \leq \frac{1}{5} C_1(q)$, $T \simeq T_{isotr}$ (see Eq. (18)).

Figure 2 illustrates the velocity distributions for these two cases and different μ . The case $v_s \ll v_e$ is actually a free-fall case whereas for the hot gas $v_s \simeq v_e$ the velocity gradient is significantly lower due to the influence of the repulsive force of gas pressure. As one can see from Figure 2, in both cases v rapidly increases as $\mu \rightarrow 1$. At the same time, the shape of the light curve in all cases studied so far proved to be quite insensitive to the velocity distribution.

The optical depths of the gas along the line of sight towards the observer τ_1 and τ_2 for the primary and secondary components, respectively, can be written down as follows:

$$\tau_1 = \tau_0 \int_{R_1}^{R_{max}} \frac{f(r, \Delta)}{R^2} dR, \tag{22a}$$

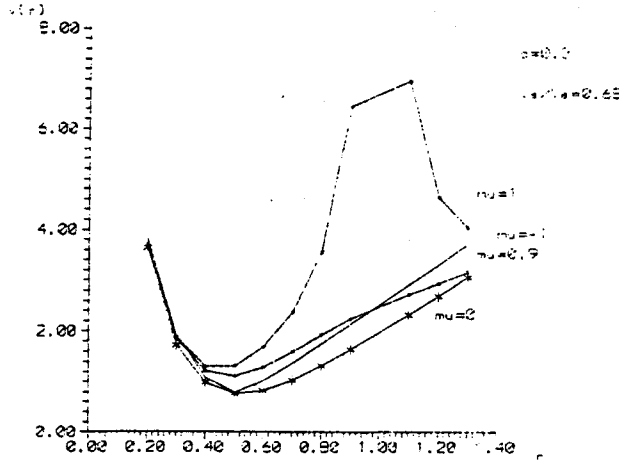


Figure 2b The same as in Figure 2a for the hot gas, $v_s/v_e = 0.65$.

$$\tau_2 = \tau_0 \int_{z_{\min}}^{z_{\max}} \frac{f(z, \Delta)}{z^2 + a^2 \Delta^2} dz. \quad (22b)$$

Here

$$R^2 = z^2 + a^2 \Delta^2, \quad \Delta = \sqrt{1 - \sin^2 i \cos^2 \phi}, \quad \tau_0 = 0.1 \frac{\dot{M}}{\pi \bar{\mu} v_k},$$

$f(r, \Delta)$, $f(z, \Delta)$ stand for the functions describing the flux tube shape and the velocity field of the stellar wind (specified by Eqs. (19) and (20), respectively), the appropriate value of the initial velocity v_k at the base of the expansion zone should be taken either from the observed chromospheric line profiles or from theoretical models of stellar wind, $\bar{\mu}$ is the molecular weight, i is the angle of orbital inclination, ϕ is the orbital phase angle measured from the moment of a superior conjunction of a primary component. Integration limits in R and z depend on the distance between the components $a\Delta$ as seen projected upon the plane of the sky,

$$R_{\max} = \begin{cases} R_A, & a\Delta \geq R_{\text{accr}}, \\ a \sin i \cos \phi + \sqrt{R_{\text{accr}}^2 - a\Delta^2}, & a\Delta \leq R_{\text{accr}}, \cos \phi > 0, \end{cases}$$

$$z_{\min} = \begin{cases} R_2, & a \sin i \cos \phi \leq R_2, \\ R_2 + a \sin i \cos \phi, & a \sin i \cos \phi > R_2, \cos \phi > 0, \end{cases}$$

$$z_{\max} = \begin{cases} R_{\text{accr}}, & a \sin i \cos \phi \leq R_2, \\ R_{\text{accr}} + a \sin i \cos \phi, & a \sin i \cos \phi > R_2, \cos \phi > 0, \end{cases}$$

$$z_{\min} = \begin{cases} R_2 - a |\sin i \cos \phi|, & a\Delta > R_A, \cos \phi < 0, \\ R_2 - a |\sin i \cos \phi|, & a\Delta < R_A, \cos \phi < 0, \end{cases}$$

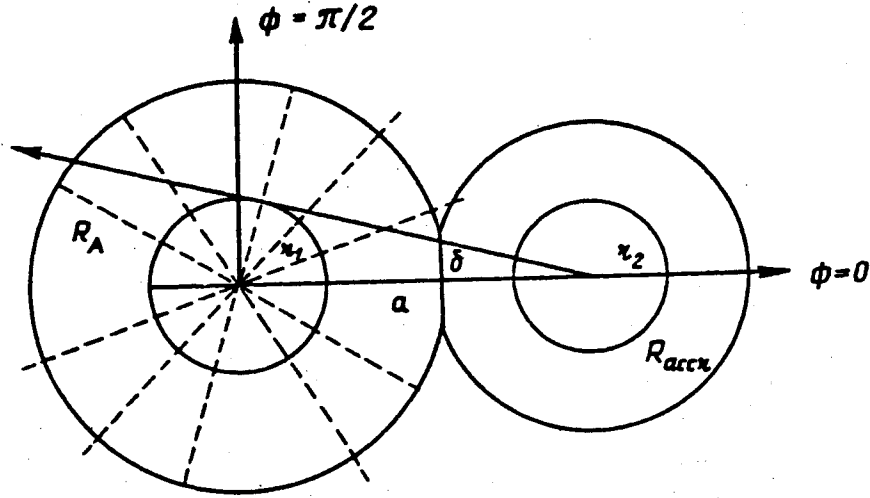


Figure 3 A schematic model of a close binary. The component of radius r_1 loses mass due to anisotropic stellar wind, R_{accr} is the accretion radius (tabulated in Table 1 in the units of a semi-major axis of a relative orbit a).

$$z_{\text{max}} = \begin{cases} R_{\text{accr}} - a|\sin i \cos \phi|, & a\Delta > R_A, \cos \phi < 0, \\ \sqrt{R_A^2 - a^2\Delta^2}, & a\Delta \leq R_A, \cos \phi < 0, \end{cases}$$

For the sake of simplicity consider the case when the anisotropy of the stellar wind is absent and the gas velocity along the line of sight is constant. We compare for this case the optical depths at elongation and during superior conjunctions. Performing integrations in (22a) and (22b) we have simple relations

$$\tau_1(\phi = \pi/2) = \tau_0 \left(\frac{1}{R_1} - \frac{1}{R_A} \right), \quad (23a)$$

$$\tau_1(\phi = 0) = \tau_0 \left[\frac{1}{R_1} - \frac{1}{a \sin i + \sqrt{R_{\text{accr}}^2 - a^2 \cos^2 i}} \right], \quad (23b)$$

$$\tau_2(\phi = \pi/2) = \frac{\tau_0}{a} \left(\arctan \frac{R_{\text{accr}}}{a} - \arctan \frac{R_2}{a} \right), \quad (23c)$$

$$\tau_2(\phi = \pi) = \frac{\tau_0}{a \cos i} \left(\arctan \frac{\sqrt{R_A^2 - a^2 \cos^2 i}}{a \cos i} + \arctan \frac{a \sin i - R_2}{a \cos i} \right). \quad (23d)$$

As one can see from Eqs. (23a), (23b), (23c) and (23d) the value of τ_1 does not change within the phase angle interval $(\pi/2, \pi)$ and only slightly increases in the phase angle interval $(0, \pi/2)$ since the density of gas rapidly declines with distance from the mass losing component. On the contrary, for the mass gaining star τ_2 is steadily increasing and for i close to 90° may be by up to 2–3 orders of magnitude

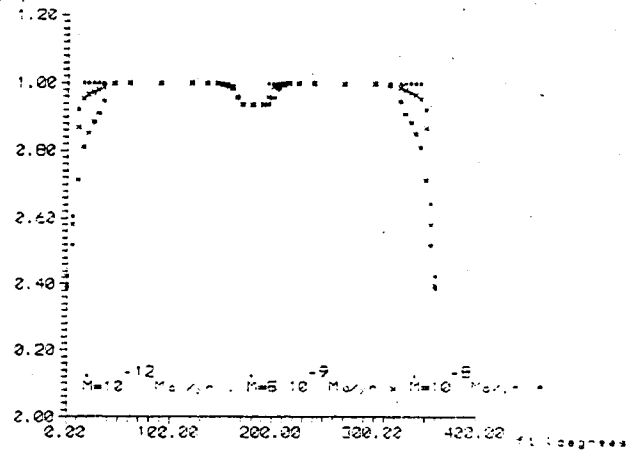


Figure 4 Model light curve of an eclipsing binary illustrating the effect of anisotropic stellar wind with the mass loss rates $\dot{M} = 10^{-12} M_{\odot} / \text{yr}$, $\dot{M} = 5 \cdot 10^{-9} M_{\odot} / \text{yr}$ and $\dot{M} = 10^{-8} M_{\odot} / \text{yr}$ for the following set of orbital elements and physical parameters: $T_{\text{eff1}} = 6000\text{K}$, $T_{\text{eff2}} = 12000\text{K}$, $r_1 = 2.2R_{\odot}$, $r_2 = 0.88R_{\odot}$, $a = 10R_{\odot}$, $i = 85^{\circ}$, $q = 1$, $\lambda = 5500\text{\AA}$ and $u_1 = u_2 = 0$.

higher compared with the value at elongation. This effect can easily explain the distortion of one of the branches of the deep minimum observed in some Algol binaries and thus it can be attributed to the effect of anisotropy of the stellar wind coming from the Roche lobe filling low mass components.

The total light of a binary (normalized to the brightness at elongation, i.e., for $\phi = 90^{\circ}$) is given by

$$\begin{aligned} L_{\lambda}(i\phi) &= L_{1\lambda}(i\phi) + L_{2\lambda}(i\phi) + L_{\text{env}}, \\ L_{j\lambda}(i\phi) &= \pi r_j^2 B_{j\lambda}(T_j) (1 - u_j/3) [1 - \Delta_j(i\phi)] \exp -\tau_j(i\phi), \end{aligned} \quad (24)$$

where $L_{j\lambda}$ is the luminosity of the respective component j with a due account for an eclipsed portion $\Delta_j(i\phi)$ of the visible disc. Here $B_{j\lambda}$ is the Planck function, and u_j is the limb darkening coefficient. The luminosity of the envelope L_{env} has been evaluated as the radiative energy of both components scattered by the envelope averaged over the orbital period,

$$L_{\text{env}} = \frac{1}{m} \sum_{m=1}^n \sum_{j=1}^2 (1 - u_j/3) \pi r_j^2 B_{j\lambda}(T_j) (1 - \Delta_{jm}) [1 - \exp -\tau_{jm}(i, \phi)], \quad (25)$$

m being the number of points or phase angle values for which the model light curves have been calculated.

The shape of the light curve is fully determined by the model parameters T_{eff1} , T_{eff2} , r_1 , r_2 , i and τ_0 or \dot{M} , q , u_1 , and u_2 . The effect of anisotropic stellar wind upon the light curve is illustrated in Figure 4 for one of the model light curves

with the physical parameters and orbital elements typical of Algol-type binaries and three values of the mass loss rate. For $\dot{M} = 10^{-12} M_{\odot} / \text{yr}$ the light curve is practically indistinguishable from the light curve of an eclipsing binary in the absence of circumstellar gas. As one can see from Figure 4, for $\dot{M} = 5 \cdot 10^{-9} M_{\odot} / \text{yr}$ and $v_{\infty} \sim 100 \text{ km/s}$ the increase by a factor of two in the mass loss rate results in a decrease by 7 per cent of the ratio of the depths of minima.

The above model has been applied by Polushina and Pustyl'nik (1994) for a detailed analysis of numerous UBV light curves of SZ Camelopardalis – an early type detached binary.

The author expresses his gratitude to Prof. A. Sapar for fruitful suggestions and encouragement and to Mrs. A. Tootsi for her help in preparing the final computer version of the manuscript.

References

- Basko, M. M. and Sunayev, R. A. (1973) *Ap. Space Sci.* **23**, 117.
 Castor, J., Abbott, D., and Klein, R. (1975) *Astrophys. J.* **195**, 157.
 Fusheng Chen (1989) *Ap. Space Sci.* **161**, 11.
 de Aranjó, F. X. and de Freitas Pacheco, J. A. (1989) *M.N.R.A.S.* **241**, 543.
 Friend, D. B. and Castor, J. I. (1982) *Astrophys. J.* **261**, 293.
 Hadrava, P. P. (1987) *Publ. Astron. Inst. Czech.* **70**, 263.
 Haisch, B. M., Linsky, J. L. and Basri, G. S. (1980) *Astrophys. J.* **235**, 519.
 Ivanov, L. (1987) *Astrofizika* **27**, 1 (in Russian).
 Kaitchuck, R. H. and Honeycutt, B. K. (1982) *PASP* **54**, No. 559, 532.
 Kaitchuck, R. H. (1989) In: *Algols*, ed. Batten A. H., Dordrecht, 51.
 Kolychalov, P. L. and Sunyaev, R. A. (1979) *Pis'ma Astron. Zh.* **5**, No. 7, 338.
 Kopp, R. A. and Holzer, T. E. (1976) *Solar Physics* **46**, 43.
 Lubow, S. H. and Shu, F. H. (1975) *Astrophys. J.* **198**, 383.
 Mazzali, F. A. (1991) *Astron. Astrophys.* **288**, 191.
 Meyer, E. and Meyer-Hofmeister, E. (1983) *Astr. Astrophys.* **121**, 29.
 McCray, R. and Hatchett, S. (1975) *Astrophys. J.* **199**, 196.
 Mihalas, D. (1978) *Stellar Atmospheres*, Freeman and Co. Publ.
 Modisette, J. and Kondo, Y. (1980) *Astrophys. J.* **240**, 180.
 Peters, G. J. (1989) In: *Algols*, ed. Batten A. H., Dordrecht, 9.
 Plavec, M. J. and Kratochvíl, P. (1964) *BAC* **217**, 775.
 Polushina, T. S. and Pustyl'nik, I. (1994) *Transactions of Soviet Astronomical Society* (the same volume).
 Svetchnikov, M. A. (1986) *Catalogue of Orbital Elements, Masses and Luminosities of Close Binary Stars*, ed. A. Dudorov, Irkutsk (in Russian).
 Tout, C. A. and Hall, D. S. (1991) *M.N.R.A.S.* **253**, 9.